Applied Catalysis B: Environmental 84 (2008) 505–513

Contents lists available at ScienceDirect

Applied Catalysis B: Environmental

journal homepage: www.elsevier.com/locate/apcatb

Co–ZSM-5 catalysts in the decomposition of N_2O and the SCR of NO with CH_4: Influence of preparation method and cobalt loading

Pieter J. Smeets, Qingguo Meng, Steven Corthals, Hugo Leeman, Robert A. Schoonheydt *

Center for Surface Chemistry and Catalysis, K.U. Leuven, Kasteelpark Arenberg 23, B-3001 Leuven, Belgium

ARTICLE INFO

Article history:
Received 26 February 2008
Received in revised form 6 May 2008
Accepted 10 May 2008
Available online 18 May 2008

Keywords:
Co–ZSM-5
Nitrous oxide decomposition
Selective catalytic reduction
SCR of NO with CH_4
Co loading

ABSTRACT

Co–ZSM-5 prepared via different methods with Co/Al ratios ranging from 0.03 to 0.83 are investigated in both the direct N_2O decomposition and the selective catalytic reduction (SCR) of NO with CH_4. UV–vis and H_2-TPR are used to get an insight in the active species in these reactions. It is observed that in catalysts with low Co loadings (Co/Al < 0.3) Co is predominantly present as mono-atomic Co species, located at ion exchange positions in ZSM-5. Higher Co loadings result in the formation of different kinds of Co-oxides, which constitute the majority of species in the over-exchanged catalysts (Co/Al > 0.5). The mono-atomic species show the highest activity in the direct decomposition of N_2O, whereas the oxidic Co species do not seem to contribute much to the overall decomposition. In the SCR, the Co-oxide species catalyze the combustion of CH_4 whereas the selectivity towards NO reduction is much increased at low Co loadings. Therefore, over-exchange of Co–ZSM-5 does not seem to be favorable for both the direct N_2O decomposition and the SCR of NO with CH_4. Co/Al ratios <0.3 give the best results both in terms of conversion and activity per Co atom in both reactions.

1. Introduction

Due to the harmful impact of NO and N_2O on the environment, researchers have investigated several ways to reduce the emission of these compounds into the air. Since the pioneering work of Iwamoto et al. [1] on the catalytic removal of NO and N_2O, many research groups have focused on the removal of these molecules. Both the direct decomposition into harmless N_2 and O_2 and the selective catalytic reduction (SCR) in the presence of short hydrocarbons, NH_3 or urea have been extensively investigated with transition metal ion (TMI)-exchanged zeolites as catalysts [2–8]. Co-zeolites have been found to be active in these reactions [9–16]. In case of the SCR of NO, the use of CH_4 as a reductant has often been proposed. It was first reported by Li and Armor [14], and has attracted great interests as it is present in almost all combustion exhausts. In addition, when compared with NH_3-SCR the CH_4-SCR offers particular advantages such as transportation, storage, equipment corrosion, etc.

For the preparation of Co-zeolites different methods were developed, often resulting in over-exchange of zeolites with Co (Co/Al > 0.5) [10,17–24]. Whereas consensus about the good activity of these Co-zeolites has been attained, the nature of the active site is still a matter of debate. Based on UV–vis, TPR, EPR, FTIR, Raman and XRD studies, Co^{2+} [17,23,25,26] Co^{3+} [27–29] and Co^0 [30–32], either mono-atomic [20,33] or multinuclear, clustered Co [23,27,34–36] have been suggested to be involved in the SCR of NO.

In the present work, different methods are used to introduce Co into ZSM-5. In this way, Co–ZSM-5 samples with Co/Al ratios ranging from 0.03 to 0.83 are obtained. The activity of these samples in both the direct decomposition of N_2O and the CH_4-SCR of NO are investigated and it is shown that the intrinsic activity per Co atom is the largest at low Co loadings in both reactions. UV–vis and TPR data are recorded and compared with literature. From this comparison it can be seen that the activity of mono-atomic Co species, located at ion exchange positions is higher than the activity of Co-oxo species.

Since in most studies on Co-zeolites the focus is on highly loaded Co-zeolites, containing various Co species, the difference between spectator sites and the actual active site is not always trivial and might explain the different conclusions obtained in the literature on Co-zeolites. The comparison of different studies is difficult as different reaction conditions and parent zeolites are used. Therefore, we prepared a large set of Co–ZSM-5 catalysts, varying in Co loading and in method of preparation and tested them under identical conditions.

* Corresponding author. Tel.: +32 16 321592; fax: +32 16 321998.
E-mail address: robert.schoonheydt@biw.kuleuven.be (R.A. Schoonheydt).

0926-3373/$ – see front matter © 2008 Elsevier B.V. All rights reserved.
doi:10.1016/j.apcatb.2008.05.002

2. Experimental

Commercial Na–ZSM-5 (Si/Al = 12, supplied by Süd-Chemie) was first ion-exchanged with an aqueous $NaNO_3$ solution overnight at ambient temperature. Cobalt acetate tetrahydrate (Aldrich, >98%) and cobalt nitrate hexahydrate (Aldrich, >98%) were used as the Co^{2+} sources. Co–ZSM-5 samples were prepared using the following methods, which are described in further detail below: wet ion exchange (WIE), ion exchange with a buffered solution (BUF), semi-continuous ion exchange (SMI) and impregnation (IMP). For convenience, the catalysts are denoted as WIE-*x*, BUF-*x*, IMP-*x* or SMI-*x*, where *x* is the Co loading expressed as the Co/Al ratio. The Co loading was determined by ICP after dissolution of the catalysts in HF.

2.1. Wet ion exchange (WIE)

This is the traditional ion exchange method. For 1 g of Na–ZSM-5, deionized H_2O was used with 1 g of the $NaNO_3$ salt. The mixture was stirred at room temperature for 24 h, filtered and washed. After the Na^+ exchange, the samples were dried at 60 °C. Subsequently six samples were prepared by adding 1 g hydrated Na–ZSM-5 to a 250 ml Co^{2+} solution with a Co concentrations of 0.05, 0.5, 1.0, 1.5 and 2 mM resulting in the catalysts WIE-0.03, WIE-0.12, WIE-0.23, WIE-0.28, respectively. The WIE-0.34 and WIE-0.33 were obtained in the same way, except that 60 ml Co^{2+} solution was used with 8.0 and 16 mM concentration. This procedure was repeated three times. In all cases ion exchange was performed for 24 h at room temperature. After ion exchange the sample was washed and dried at 110 °C.

2.2. Buffered ion exchange (BUF)

The same procedure is used as in the WIE method, except that the exchange solution was buffered at pH 8. 1 g of Na–ZSM-5 was mixed with 60 ml of a 0.5 and 16 mM Co^{2+} solution resulting in the catalysts BUF-0.11 and BUF-0.41, respectively. The Co^{2+} exchange was repeated three times for BUF-0.41. The filtration, washing and drying procedures were the same as for the WIE samples.

2.3. Impregnation (IMP)

To 1 g of Na–ZSM-5 1.7 ml deionized water containing the necessary amount of Co^{2+} to obtain initial Co/Al ratios of 0.1 and 0.85 were added for the impregnation. The mixture was thoroughly mixed for 24 h. The impregnated samples were dried in air at 100 °C overnight and calcined at 450 °C for 10 h. The thus obtained catalysts are denoted as IMP-0.10 and IMP-0.83.

2.4. Semi-continuous method (SMI)

Samples SMI were prepared according to the method of [20,24]. Na–ZSM-5 was mixed with 45 ml water under stirring at 80 °C. 15 ml aqueous solutions of cobalt acetate with Co concentrations of 8 and 64 mM were added drop-wise at a rate of 1 ml/min under reflux at 80 °C, resulting in SMI-0.30 and SMI-0.78, respectively. After refluxing for 24 h the catalysts were filtered. This ion-exchange procedure was repeated three times for SMI-0.78. After this procedure the same filtration, washing and drying procedure was followed as for the WIE catalysts.

2.5. Catalytic activity measurement

Catalytic activity of 0.2 g catalyst (pellets of 0.25–0.5 mm) was examined in the decomposition of N_2O and NO in a plug-flow reactor. The catalysts were calcined overnight at 450 °C (with heating ramp of 1 °C/min) in a He flow (50 ml/min) before catalytic reactions. For the N_2O decomposition, the inlet gas was 0.5 vol.% N_2O balanced with He resulting in a total flow of 100 ml/min. The GHSV was about 15,000 h^{-1} (based on the ZSM-5 density = 0.5 g/ml). In the case of SCR-NO the inlet gas was composed of 0.5 vol.% NO, 1.0 vol.% CH_4 and 5.0 vol.% O_2 balanced with He. The total flow was 20 ml/min and the GHSV was 3000 h^{-1}.

A HP 4890D gas chromatograph (GC) equipped with a TCD detector was used to monitor N_2, CH_4, N_2O and O_2. The N_2O and NO conversion were calculated on the basis of the yield of N_2 according to Eqs. (1) and (2), respectively. The methane conversion was calculated from its total consumption, Eq. (3). Additionally, the formation of N_2 and O_2 was analyzed online with an Omnistar quadrupole mass-spectrometer (QMS 200) upon switching from a He flow to a 0.5% N_2O flow at 300 °C over a WIE-0.33 catalyst.

$$N_2O_{\text{conversion}}\,(\%) = \left(\frac{[N_2]_{\text{outlet}}}{[N_2O]_{\text{inlet}}}\right) \times 100 \quad (1)$$

$$NO_{\text{conversion}}\,(\%) = 2\left(\frac{[N_2]_{\text{outlet}}}{[NO]_{\text{inlet}}}\right) \times 100 \quad (2)$$

$$CH_{4\ \text{conversion}}\,(\%) = \left(\frac{1 - [CH_4]_{\text{outlet}}}{[CH_4]_{\text{inlet}}}\right) \times 100 \quad (3)$$

2.6. Characterization

In situ UV–vis–NIR spectra of the Co catalysts were recorded in the diffuse reflectance mode (DRS) on a Varian Cary 5 UV–vis-NIR spectrophotometer. The samples (pellets of 0.25–0.5 mm) were brought into quartz flow cells, with a suprasil window for DRS measurements. After overnight calcination (heating rate of 1 °C min^{-1} to 450 °C; 100% O_2, flow of 50 ml min^{-1}), the samples were cooled in a closed O_2 atmosphere and measured at room temperature. The spectrum of a white reference polymer was subtracted from all spectra.

H_2-TPR experiments were carried out using an OmnistarTM gas analysis system (Pfeiffer vacuum). The catalysts were pretreated in oxygen at 450 °C. After cooling to room temperature, 5 vol.% H_2/N_2 (12 ml min^{-1}) was introduced in the system and the temperature was increased to 980 °C at a heating rate of 10 °C min^{-1}. The consumption of H_2 was analyzed online with an Omnistar quadrupole mass-spectrometer (QMS 200).

3. Results and discussion

3.1. Co loading in ZSM-5 by different methods

Table 1 gives the different catalysts with their Co loading, expressed in weight percentage and in Co/Al ratios. With the classical ion exchange method (WIE) six samples with increasing Co loading were prepared. The maximum loading that could be achieved was 2.4 wt.%. The Co/Al ratio is then 0.34 corresponding to 68% of the cation exchange capacity (CEC).

To obtain higher Co loadings we have performed three other techniques: exchange in a buffered solution at pH 8; exchange under reflux and impregnation. Table 1 shows that indeed higher loadings of cobalt can be achieved and that over-exchanged ZSM-5 can be obtained by impregnation (IMP-0.83) and by reflux (SMI-0.78). For the sample BUF-0.41 the Co loading corresponds to 82% of the exchange sites, using the same initial Co concentration as the WIE-0.33 catalyst. The higher loading of BUF-0.41 can be ascribed to the increased pH, resulting in the exchange of $[Co(OH)]^+$ as

Table 1
Composition and characterization of the Co–ZSM-5 catalysts

Catalyst[a]	Ion exchange temperature (°C)	Co content (wt.%)	Co/Al
SMI-0.78	80	5.5	0.78
SMI-0.30	80	2.1	0.30
BUF-0.41	25	2.9	0.41
BUF-0.11	25	0.8	0.11
IMP-0.83	25	5.8	0.83
IMP-0.10	25	0.7	0.10
WIE-0.33	25	2.3	0.33
WIE-0.34	25	2.4	0.34
WIE-0.28	25	2.0	0.28
WIE-0.23	25	1.6	0.23
WIE-0.12	25	0.8	0.12
WIE-0.03	25	0.2	0.03

[a] The catalysts are denoted as WIE-*x*, BUF-*x*, IMP-*x* or SMI-*x*, where *x* is the Co loading expressed as the Co/Al ratio. WIE represents the catalysts prepared via the wet ion-exchange method, IMP those prepared via impregnation, BUF catalysts are prepared via ion exchange with a buffered solution and SMI via a semi-continuous ion exchange.

reported in [37]. We have performed spectroscopic measurements and H_2-TPR to get insight in the state of cobalt in the catalysts.

3.2. Catalyst characterization

The UV–vis spectra of the calcined WIE catalysts are shown in Fig. 1a. They are typical for isolated, mono-atomic Co^{2+} in ZSM-5 [26,29,34,38–43]. The d–d transitions are visible as two triplets: one in the NIR and one in the visible. The former is weak and comprises bands at 5000 cm^{-1}, 6500 cm^{-1} and 8000 cm^{-1}. Two sharp bands at 4570 cm^{-1} and 7180 cm^{-1} are superposed on this NIR triplet. They are assigned, respectively to the $(\nu + \delta)$ combination band and 2ν overtone band of the silanols and/or bridging OH groups. The band maxima of the triplet in the visible region are located at 15,000 cm^{-1}, 17,750 cm^{-1} and 20,850 cm^{-1}. The latter band is absent at the lowest Co loading (WIE-0.03). Wichterlova and coworkers have interpreted these spectra in terms of Co^{2+} at three different sites in the ZSM-5 channel system [38,40]. Pierloot et al. have shown that the number of Al tetrahedra, which form a site (six-rings, five-rings), is also important [44]. In any case, the absence of the 20,850 cm^{-1} band at the lowest Co loading and the increasing intensity at higher Co loading indicates the presence of at least two different Co^{2+} species.

The spectra of the catalysts prepared with the other methods are shown in Fig. 1b. For Co/Al ratios below 0.5 the spectra are very similar to those of the WIE samples. In general, however, the triplet in the NIR is less resolved, especially the 5000 cm^{-1} band. In the visible region of the spectra the 20,850 cm^{-1} band is well resolved for IMP-0.10, SMI-0.30 and BUF-0.41, much less so for BUF-0.11. The over-exchanged samples are characterized by a broad band between 22,000 cm^{-1} and 28,000 cm^{-1}. In the case of IMP-0.83 the spectrum is very characteristic with a new band at 13,300 cm^{-1} and a band at 6400–8000 cm^{-1} in the NIR. Such a spectrum is typical for Co_3O_4 particles, but some CoO clusters may be present too (d–d bands at 8000 cm^{-1} and 19,600 cm^{-1}). The latter is evidenced by the 8000 cm^{-1} shoulder on the 6400 cm^{-1} band [45,46].

Typical H_2-TPR data are depicted in Fig. 2. Two regions of H_2 consumption are visible. The high temperature region (675–900 °C) is present in all catalysts. H_2 consumption in this region is due to reduction of mono-atomic Co^{2+} on ion exchange sites [22,23]. In the catalysts with the low Co loadings, only the high temperature reduction peaks are observed. The low temperature regime (220–500 °C) is visible for the catalyst with high Co loadings (Co/Al > 0.25) and the over-exchanged catalysts. For WIE-0.33, a reduction peak at about 450 °C emerges which can be ascribed to CoO, whereas the peak at 200–350 °C in SMI-0.78 can be ascribed to the reduction of Co_3O_4 [17,29,47]. These TPR data qualitatively agree with the UV–vis data: mono-atomic Co atoms are observed in all catalysts and at increasing Co loading, additional Co species are formed, like CoO and Co_3O_4.

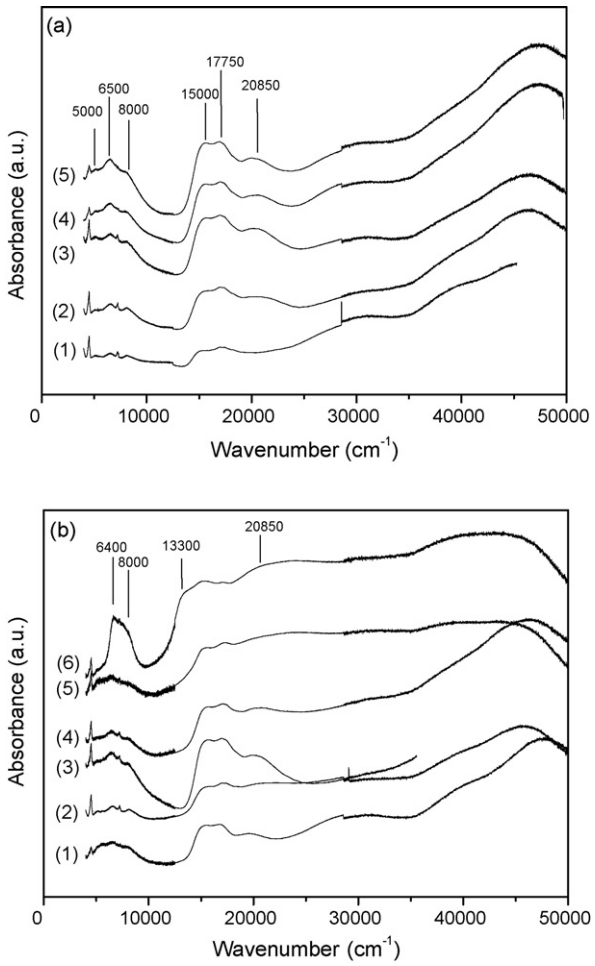

Fig. 1. (a) UV–vis spectra of Co–ZSM-5 prepared via the WIE method of (1) WIE-0.03, (2) WIE-0.12, (3) WIE-0.23, (4) WIE-0.28 and (5) WIE-0.34; (b) UV–vis spectra of Co–ZSM-5 prepared via the other methods: (1) IMP-0.10, (2) BUF-0.11, (3) SMI-0.30, (4) BUF-0.41, (5) SMI-0.78 and (6) IMP-0.83.

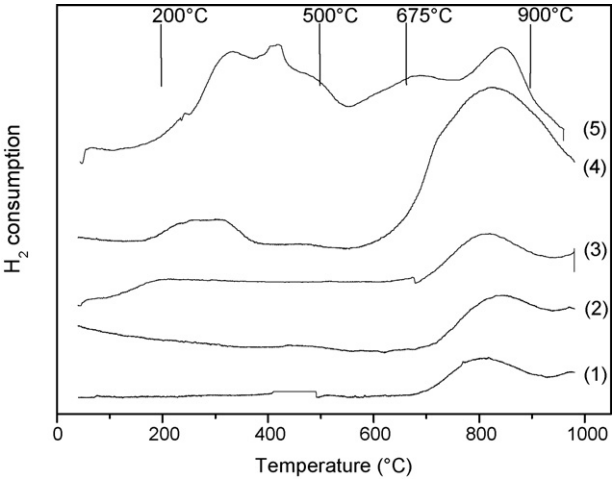

Fig. 2. H_2-TPR (5 vol.% H_2) profile of (1) WIE-0.23, (2) WIE-0.34, (3) BUF-0.41, (4) SMI-0.78 and (5) IMP-0.83 as a function of temperature.

3.3. N_2O decomposition over Co–ZSM-5 catalysts

3.3.1. Direct N_2O decomposition

The activity of the Co–ZSM-5 samples in the direct decomposition of N_2O (0.5 vol.%) was subsequently tested and the conversion data and turn-over-frequencies (TOFs) as a function of reaction temperature are reported in Fig. 3a–d. For the ion-exchanged catalysts (WIE) the conversion increases steadily with the Co^{2+} loading [48]. However, comparing the activity per Co atom (TOF), the TOFs are almost independent of the Co content of the catalysts. At temperatures higher than 425 °C, the conversion over the catalysts with the highest Co loading approach 100%, explaining the leveling off of the TOFs. These data confirm that isolated Co^{2+} atoms in ion exchange positions are active in the direct decomposition of N_2O in the temperature region 350–450 °C.

The conversion and TOF as a function of temperature over the Co–ZSM-5 catalysts prepared via the BUF, SMI and IMP method are reported in Fig. 3b and d. The conversion curves for most catalysts fall close to each other and conversions of 100% are reached above 425 °C. Only for IMP-0.10 and BUF-0.11 the conversions are significantly lower. However, in terms of TOF (Fig. 3d) another picture emerges. The catalysts with Co/Al < 0.5 (except IMP-0.10) clearly show a higher TOF than the over-exchanged catalysts and IMP-0.10. The TOFs of BUF-0.10, SMI-0.30 and BUF-0.41 are comparable to the TOFs of the WIE catalysts. In these catalysts, as for the catalysts prepared via WIE, the predominant Co species are mono-atomic Co as evidenced by the UV–vis spectra and TPR results. Hence, the activity in the decomposition of N_2O can be largely ascribed to these species, and is independent of the ion-exchange method. In the over-exchanged catalysts, a large fraction of the Co is present in oxidic clusters. Their activity per Co atom is much less because probably not all the Co atoms are available for reaction and the intrinsic activity of the Co atoms in these oxidic species might be lower than that of the mono-atomic Co ions in exchange positions.

Co–ZSM-5 catalysts clearly behave differently from Cu-zeolites in the direct decomposition of N_2O. Cu-catalysts with Cu/Al <0.25 show very low activity, whereas at increasing Cu/Al ratios, the TOF is greatly increased [49,50]. The lack of such a jump in TOF over the Co–ZSM-5 catalysts suggests a different reaction mechanism over Cu- and Co-zeolites. Over Cu zeolites, a clear correlation between the activity in the N_2O decomposition and Cu density in the zeolite is observed [50,51]. At low Cu loading (Cu/Al < 0.25), most Cu sites are isolated as evidenced with EPR [50,52]. As one oxygen atom is deposited by N_2O on a Cu site, these deposited oxygen atoms are also isolated from each other. Hence migration of oxygen atoms is required before molecular oxygen can desorb, which is the rate limiting step in the N_2O decomposition over Cu-zeolites. As the Cu density increases, this migration step is less hindered resulting in an increased activity at higher Cu loadings. In Cu–ZSM-5 catalyst, the deposition of two oxygen atoms on neighboring sites results in the formation of a Cu dimer bridged by two oxygen atoms. From this Cu dimer core, molecular oxygen can desorb without a migration step, explaining the superior activity of the Cu–ZSM-5 catalysts with Cu/Al >0.25 [49–51].

The literature on Fe-zeolites does not give such a clear picture as that of the Cu-zeolites. This is because of the large variety of Fe species which all contribute to the overall N_2O decomposition although to a different extent [53–56]. Often a high initial activity is observed that decays to a lower steady-state activity. In a recent study of Pirngruber this is addressed [57]. The initial high activity of Fe–ZSM-5 is often attributed to a transient activity over dehydroxylated Fe sites, which slowly loose there activity due to small traces of H_2O in the reaction feed. Once steady-state is reached, the contribution of an O-migration step is often reported to be involved in the decomposition of N_2O, similar to Cu-zeolites.

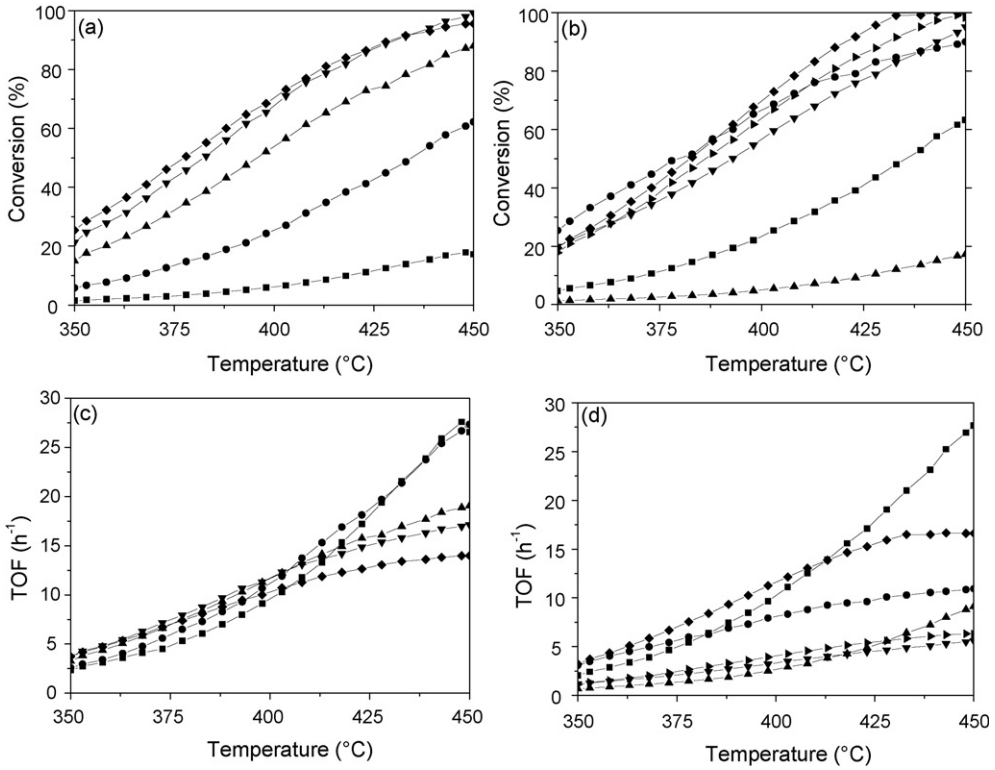

Fig. 3. Conversion (a) and TOF (c) of 0.5 vol.% N_2O over (■) WIE-0.03, (●) WIE-0.12, (▲) WIE-0.23, (▼) WIE-0.28, (◆) WIE0.34; conversion (b) and TOF (d) of 0.5 vol.% N_2O over (■) BUF-0.11, (●) BUF-0.41, (▲) IMP-0.10, (▼) IMP-0.83, (◆) SMI-0.30 and (▶) SMI-0.78.

Table 2
Conversion of N_2O (%) and reaction rate as a function of N_2O concentration (vol.% in 100 ml/min He flow) at 420 and 470 °C over WIE-0.03

N_2O inlet concentration (vol.%)	Conversion at 420 °C (%)	Rate at 420 °C ($\times 10^{-5}$)	Conversion at 470 °C (%)	Rate at 470 °C ($\times 10^{-5}$)
0.15	9	0.39	25	1.0
0.25	8	0.62	24	1.8
0.5	9	1.4	24	4.0
1	9	2.7	24	7.4
1.5	9	4.0	25	12
2	9	5.7	25	16

Since the isolated Co species in WIE-0.03 show already good activity in the N_2O decomposition, the recombinative O_2 desorption is not the dominant mechanism for the decomposition of N_2O. The present data suggest that two N_2O molecules react on one Co site, opposite to one N_2O per Cu site. This can be accomplished via a single site (R2) or an Eley–Rideal (R3) like mechanism. Kapteijn et al. [13] interpreted their data for Co–ZSM-5 in terms of an Eley–Rideal mechanism which is in line with the present results. This mechanism would result in a first order in N_2O as reported in the work of Kapteijn et al. Therefore, the conversion of N_2O over WIE-0.03 was investigated at 420 °C and 470 °C as a function of N_2O inlet concentration. The conversion data and the corresponding rates are given in Table 2. In Fig. 4, the ln(rate) vs. ln(N_2O conc.) is plotted, from which the order in N_2O can be attained. At both temperatures, a first order in N_2O is observed. Whereas partial orders in N_2O are reported for Cu-zeolites (between 0.3 and 0.7) [51], this is an additional line of evidence for a different mechanism for Co–ZSM-5 as compared to Cu-zeolites. This mechanism is represented by the following elementary steps:

$$N_2O + * \rightarrow N_2 + *O \quad (R1)$$

$$O* + N_2O \rightarrow O_2* + N_2 \rightarrow O_2 + * \quad (R2)$$

$$O* + N_2O \rightarrow O_2 + N_2 + * \quad (R3)$$

with * representing an active Co site.

In order to obtain additional insight in the mechanism of N_2O decomposition the formation of N_2 and O_2 was monitored over WIE-0.33 upon switching from a He flow to a 0.5% N_2O flow at

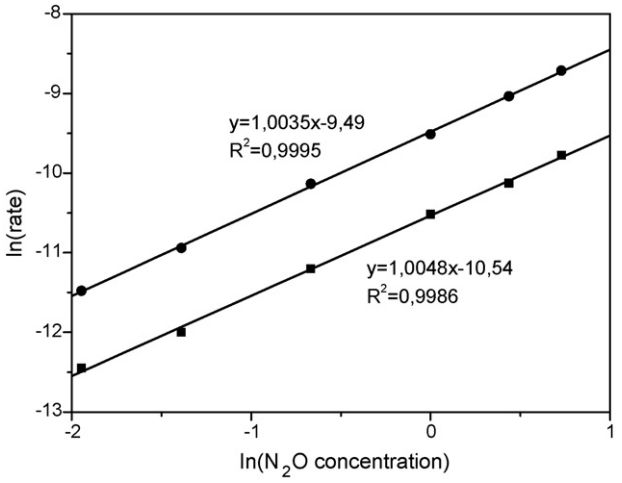

Fig. 4. The ln(rate) as a function of ln(N_2O concentration) for WIE-0.03 at (■) 420 °C and (●) 470 °C. The equation for the linear fit, as well as the R^2 is given for each temperature.

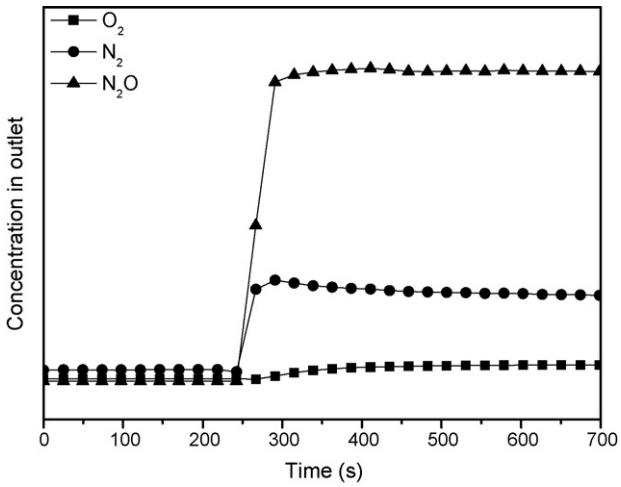

Fig. 5. Concentration of (■) O_2, (●) N_2 and (▲) N_2O during the initial stages of the N_2O decomposition (0.5 vol.% N_2O) over WIE-0.33 at 300 °C. After 250 s N_2O flow was opened.

300 °C (Fig. 5). Initially N_2 is formed and only little O_2 is detected. As the O_2 outlet concentration increases to its steady-state value, the N_2 concentration decreases slowly, indicating that initially (R1) occurs and as the surface is gradually covered with O atoms, N_2O reacts with these deposited O atoms (R3). The decreasing N_2 concentration indicates that (R3) is slower than (R1).

3.3.2. N_2O decomposition in the presence of NO, O_2 or H_2O

The influence of NO, O_2 and H_2O on the N_2O decomposition is also investigated. NO has been reported to exert a positive effect on the activity of Cu- and Fe-zeolites when, in the absence of NO, migration of O atoms is involved. O_2 has no effect on the activity of Cu- and Fe-zeolites [50,51,58]. However negative effects of O_2 have been observed over hydrotalcites [59]. Here the mechanism of N_2O decomposition was proven to be a single site mechanism ((R1) and (R2)). In that case, adsorption of O_2 competes with (R2) and decreases the overall conversion of N_2O. Generally, only negative effects of H_2O on the N_2O decomposition are reported, due to competitive adsorption between N_2O and H_2O. Recently we reported a positive effect of H_2O on the activity of Cu-zeolites with low Cu loading [51]. This was attributed to the (reversible) migration of Cu atoms, thereby decreasing the average Cu–Cu distance and hence facilitating the recombinative O_2 desorption.

In Table 3, the decomposition of N_2O in the presence and absence of NO, O_2 and H_2O is compared. NO was found to have no effect on the decomposition over WIE-0.03, although at increasing Co loading the presence of NO results in a decrease of the conversion of N_2O. This is another indication that O-migration is not involved in the N_2O decomposition over Co–ZSM-5. Apparently, the effect of NO becomes more negative at increasing Co loading as can be observed from Table 3. This negative effect decreases with increasing reaction temperature, suggesting that the negative effect of NO can be attributed to adsorption on Co species, thereby blocking the active site. Since also no effect of O_2 could be detected over the Co-zeolites investigated, the single site mechanism ((R1) followed by (R2)) can be ruled out, leaving the Eley–Rideal mechanism as the most plausible reaction mechanism. H_2O was found to have a strong negative effect on the N_2O decomposition in agreement with most literature on TMI-zeolites. In recent publications on Co–BEA [60,61] Co species were reported that do not adsorb H_2O molecules. This was achieved by calcination of the as-synthesized BEA zeolite in an ammonium stream. As the activity of Co species under dry condition is often

Table 3
Conversion of 0.5 vol.% N_2O (%) in the absence and presence of 0.1 vol.% NO, 5 vol.% O_2 and 5 vol.% H_2O at 350 °C, 400 °C and 450 °C

Catalyst	Conversion N_2O (%)			Conversion N_2O + NO (%)			Conversion N_2O + O_2 (%)			Conversion N_2O + H_2O (%)		
	350 (°C)	400 (°C)	450 (°C)	350 (°C)	400 (°C)	450 (°C)	350 (°C)	400 (°C)	450 (°C)	350 (°C)	400 (°C)	450 (°C)
WIE-0.33	25	70	99	10	44	99	24	71	99	0	0	1
WIE-0.23	15	54	87	10	48	86	15	55	86	0	1	10
WIE-0.03	2	6	18	2	6	17	1	5	16	0	1	12

reported to be higher than the activity of Fe species [5,12,13], this pretreatment method might help overcome the severe inhibition effect of H_2O on Co-zeolites and result in highly active catalysts.

From the present results, it can be concluded that the optimal Co/Al loading in ZSM-5 for the direct decomposition of N_2O is lower than 0.4. At higher Co loading, Co-oxides are formed, which appear to be spectator sites in the decomposition of N_2O. Both the highest activity per gram zeolite (conversion) and per Co atom (TOF) is attained over Co–ZSM-5 catalysts with Co/Al = 0.3–0.4, irrespective of the preparation method. Co/Al ratios lower than this optimal loading result in lower conversions but almost equal TOFs whereas over-exchanged Co–ZSM-5s (SMI and IMP) show similar conversions but lower TOFs. Over-exchange should thus be avoided.

3.4. SCR NO conversion over Co–ZSM-5 catalysts

3.4.1. NO + CH_4

The activity of the Co catalysts was investigated in the reduction of NO (0.5 vol.%) with CH_4 (1 vol.%) in the absence of O_2. The conversion data and TOFs are shown in Fig. 6a–d. Often it is reported that NO can only be reduced by CH_4 after it has been oxidized by O_2 into more reactive (sorbed or gaseous) NO_y species [23,28,62]. These figures however clearly show that reduction of NO can also occur without the NO oxidation step. Several catalysts can even reduce more than 80% of the inlet NO at 550 °C.

For the WIE catalysts the conversion increases with Co loading, and the corresponding TOFs, shown in Fig. 6c, are similar for all WIE catalysts. The exception is WIE-0.03 with a TOF which is a factor 2 higher than that of the other catalysts. However, the uncertainties on the TOFs of this catalyst are rather large due to the low conversions. The difference in TOF is probably not significant. The catalysts prepared via the other preparation methods all show conversions comparable to the WIE catalysts. A tendency towards lower TOFs for the over-exchanged catalysts can be observed (up to a factor of two smaller). This suggests that, similar to the situation in the direct N_2O decomposition, the Co sites in ion exchange positions show higher activity than the Co-oxide species.

3.4.2. NO + CH_4 + excess O_2

Addition of excess O_2 (5 vol.%) to the CH_4 + NO reaction results in the conversion curves shown in Fig. 7a–d. From these curves the following observations are made: (i) below 450 °C the conversion of NO is significantly increased as compared to the conversion in

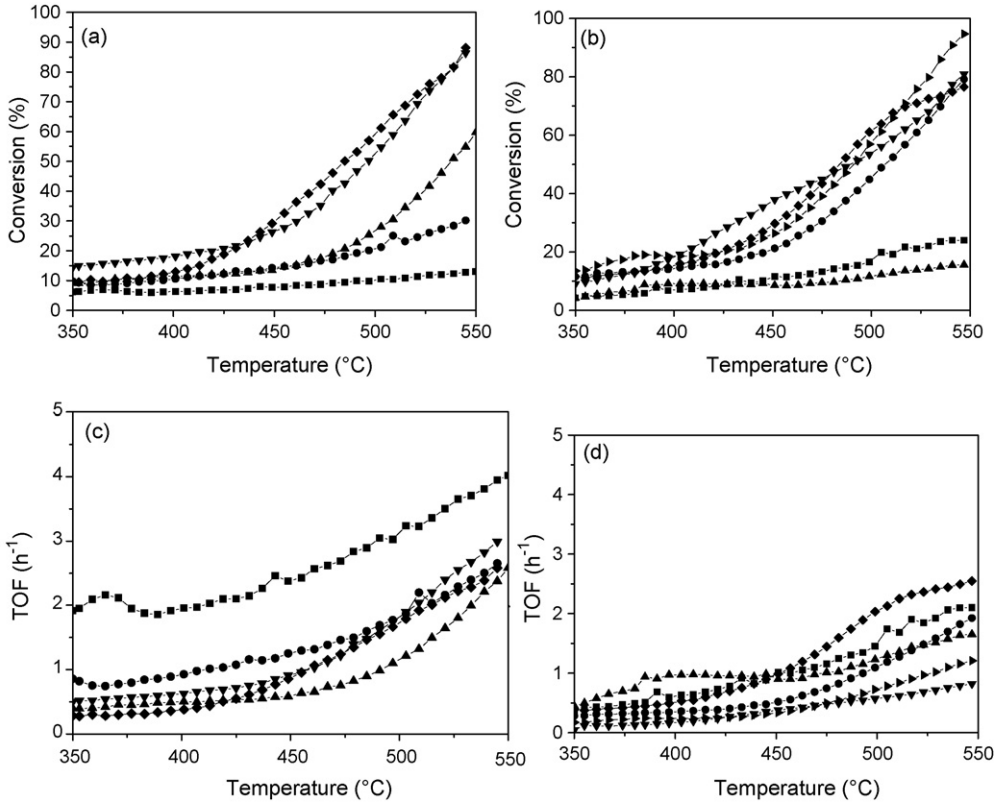

Fig. 6. Conversion (a) and TOF (c) of NO during NO (0.5 vol.%) + CH_4 (1 vol.%) treatment over (■) WIE-0.03, (●) WIE-0.12, (▲) WIE-0.23, (▼) WIE-0.28 (◆) WIE0.34; conversion (b) and TOF (d) of NO during NO (0.5 vol.%) + CH_4 (1 vol.%) over (■) BUF-0.11, (●) BUF-0.41, (▲) IMP-0.10, (▼) IMP-0.83, (◆) SMI-0.30 and (▶) SMI-0.78).

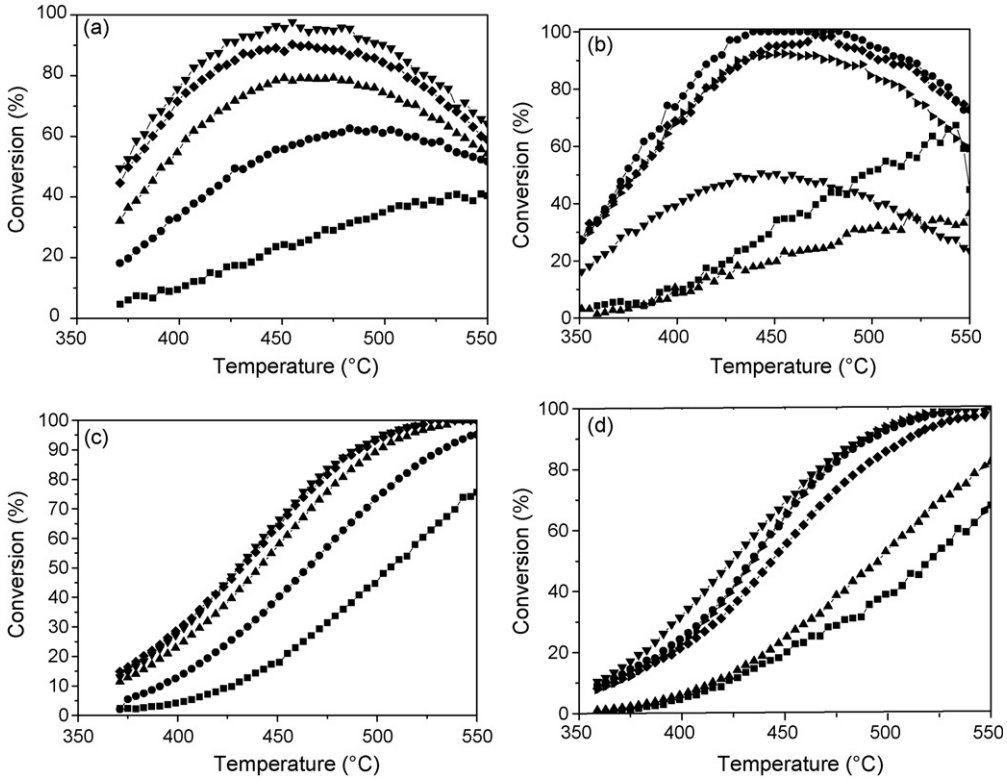

Fig. 7. (a) and (b) Conversion of NO during the SCR (0.5 vol.% NO + 1 vol.% CH_4 + 5 vol.% O_2) as a function of temperature over (a) (■) WIE-0.03, (●) WIE-0.12, (▲) WIE-0.23, (▼) WIE-0.28, (◆) WIE0.34 and (b) (■) BUF-0.11, (●) BUF-0.41, (▲) IMP-0.10, (▼) IMP-0.83, (◆) SMI-0.30, (►) SMI-0.78; (c) and (d) conversion of CH_4 during the SCR (0.5 vol.% NO + 1 vol.% CH_4 + 5 vol.% O_2) as a function of temperature over (c) (■) WIE-0.03, (●) WIE-0.12, (▲) WIE-0.23, (▼) WIE-0.28, (◆) WIE0.34 and (d) (■) BUF-0.11, (●) BUF-0.41, (▲) IMP-0.10, (▼) IMP-0.83, (◆) SMI-0.30, (►) SMI-0.78.

the absence of O_2 (see Fig. 6a and b); (ii) above 450 °C a maximum in the conversion of NO is observed for all catalysts, except those with the lowest Co^{2+} loadings (Co/Al < 0.15); (iii) at temperatures above 500 °C, the conversion of NO can even drop below the level attained in NO + CH_4 reaction in the absence of O_2; (iv) the maxima in the conversion plots tend to shift to lower temperatures with increasing Co loading; (v) the conversion of NO increases with increasing Co loading up to a Co/Al ratio of 0.4. A further increase of the Co loading, i.e. the over-exchanged catalysts, results in a decrease in NO conversion, especially for IMP-0.83; (vi) the conversion of CH_4 increases steadily with temperature and – at each temperature – it increases with Co^{2+} loading (Fig. 7c and d). Looking at the conversion curves of CH_4, it can be seen that the amount of CH_4 consumed largely exceeds the amount of NO reduced for all catalysts. Since no conversion of CH_4 is observed over the parent Na–ZSM-5 during the SCR conditions (results not shown), it can be concluded that this excess conversion of CH_4 occurs on Co sites. As often reported in the literature CH_4 is consumed via two parallel pathways, the reduction of NO_x (R4) and the combustion by O_2 (R5).

$$CH_4 + 4NO \rightarrow CO_2 + N_2 + 2H_2O \quad (R4)$$

$$CH_4 + 2O_2 \rightarrow CO_2 + 2H_2O \quad (R5)$$

At low temperatures (below 450 °C), the reduction of NO_x is dominant. At higher reaction temperatures (above 450 °C), the combustion of CH_4 takes over. Less methane is available for SCR and the conversion of NO drops, even below the conversion level attained during the NO + CH_4 reaction. The result is a maximum in the conversion of NO during SCR.

The TOFs for the NO decomposition are plotted in Fig. 8a and b. For the WIE catalysts the TOFs increase above 400 °C with decreasing Co loading. At 550 °C for example the TOF in NO for the WIE-0.03 catalyst is about 10 times higher than the TOF of WIE-0.34. A similar trend is observed for the other catalysts (Fig. 8b). At 550 °C the highest TOFs are observed for the catalysts with the lowest Co content whereas the lowest TOFs are observed for the catalysts with the highest Co content. Below 400 °C, the TOFs in NO of most catalysts are rather similar. As combustion of CH_4 becomes more dominant over Co-oxide species these trends can be understood [20,34,42,63]. The same holds for the other catalysts. As in the over-exchanged catalysts a larger fraction of oxidic Co species are present, the combustion of CH_4 starts dominating at lower temperatures. The result is a maximum in the conversion of NO at lower temperatures than for the WIE catalysts.

When the reduction of NO by methane in the presence and absence of O_2 is considered at low temperatures, the beneficial effect of O_2 over catalysts with mono-atomic Co^{2+} sites is clearly evidenced. The NO conversion below 400 °C can even increase from less than 20% up to about 80% upon adding excess O_2 over WIE-0.34. This beneficial effect of O_2 is often attributed to either an enhanced liberation of the active site (carbonaceous intermediates, like Co-isocyanate [28,64–66] are burned off, liberating the active site) or the formation of adsorbed NO_y species with a higher activity towards CH_4 [67,68]. From FTIR studies, it could be seen that upon adding CH_4 to a NO + O_2 mixture at 400 °C, the intensity of the adsorbed NO_y species strongly decreases, suggesting a reaction of CH_4 with these species [23]. An FTIR study on WIE-0.34 confirmed this reaction of CH_4 with the adsorbed NO_y species (results not shown). Whether these NO_y intermediates are formed specifically at Co^{3+} sites, as suggested by Montanari et al. [27,28],

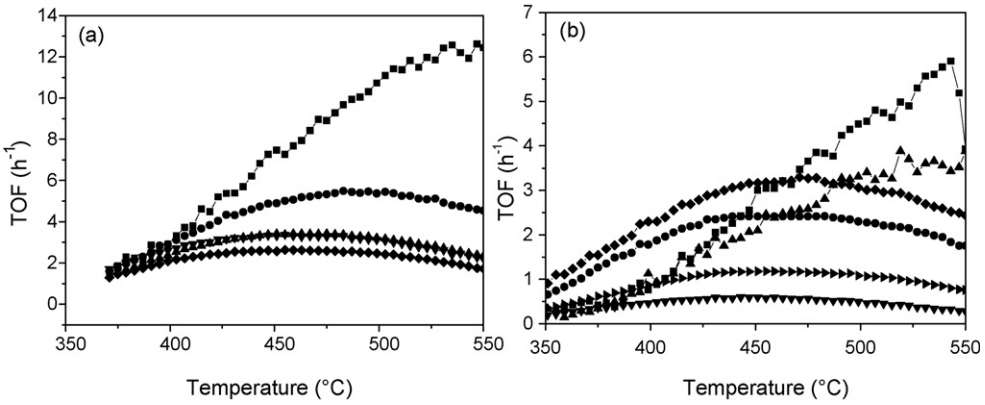

Fig. 8. TOF of NO during the SCR (0.5 vol.% NO + 1 vol.% CH_4 + 5 vol.% O_2) as a function of temperature over (a) (■) WIE-0.03, (●) WIE-0.12, (▲) WIE-0.23, (▼) WIE-0.28, (◆) WIE0.34 and (b) (■) BUF-0.11, (●) BUF-0.41, (▲) IMP-0.10, (▼) IMP-0.83, (◆) SMI-0.30, (►) SMI-0.78.

cannot be concluded from the present results. In the work of Gora-Marek et al. [69] it was shown that at increasing Co/Al ratio, or increasing presence of Co-oxides, the relative abundance of these Co^{3+} species decreases. If these sites were the only sites capable of reducing NO with CH_4, a significant decrease in TOF with increasing Co loading would be expected in the NO + CH_4 reaction. However, only for the over-exchanged catalyst a significantly lower TOF is observed in this reaction (see Fig. 6c and d). Hence the reduction of NO does not exclusively occur on these Co^{3+} sites.

In conclusion, the combustion of CH_4 is less dominant over the mono-atomic Co species at ion exchange positions, i.e. these Co sites are more selective to the reduction of NO. The best results in the SCR of NO with CH_4 below 400 °C are obtained for Co–ZSM-5 catalysts with a Co/Al <0.4. At higher temperatures, even lower Co loadings (Co/Al < 0.1) are more favorable, irrespective of the preparation method. At all temperatures, over-exchanged Co–ZSM-5 samples are not suited for SCR of NO due to the presence of large amounts of Co-oxide clusters accelerating the combustion of CH_4. Whereas in the past, the focus in the SCR of NO over Co-zeolites was on relatively high Co loading [23,24,27,29], the present study clearly shows that catalysts with low Co content are more suited at high temperatures. Additionally, it is shown that upon decreasing the Co loading in Co–ZSM-5 the temperature window for CH_4-SCR of NO can be broadened towards higher operation temperatures, whereas at higher Co loading the selectivity towards NO reduction is greatly reduced.

4. Conclusions

Co–ZSM-5 catalysts can be prepared with various Co loadings, including over-exchanged catalysts. With classical wet ion exchange (WIE) Co/Al ratios of 0.34 can be achieved and most Co is found to be positioned in ion-exchange sites. With the other preparation methods similar distribution of Co is observed at low Co loading (Co/Al < 0.30), but at higher Co loading additional oxidic Co species are being formed.

In the direct decomposition of N_2O, these mono-atomic Co species in ion exchange positions are found to be the most active sites. The reaction is first order in N_2O. This can be explained by an Eley–Rideal mechanism, as proposed by Kapteijn et al. [13]. For over-exchanged catalysts, containing large amounts of Co-oxides, the TOF dropped drastically. This suggests that in the N_2O decomposition, these species are less active or even inactive.

NO can be reduced with CH_4 to N_2 in the absence of O_2. In the presence of excess O_2 the conversion of NO is significantly increased at low temperatures over all catalysts. However for most catalysts, at 550 °C the conversion of NO drops below the conversion attained in the absence of O_2. This maximum in the conversion of NO is due to a parallel combustion of CH_4 which is more favorable at higher temperatures. Additionally, this combustion reaction occurs at lower temperatures and to a larger extent over oxidic Co species, making the over-exchanged Co–ZSM-5 catalysts less feasible catalysts for the SCR of NO with CH_4. The best results under the present reaction conditions are observed over catalysts containing only mono-atomic Co ions in ion-exchange positions, i.e. Co–ZSM-5 catalysts with Co/Al <0.15.

Acknowledgments

PJS and SC thank the Institute for the Promotion of Innovation through Science and Technology in Flanders (I.W.T.-Vlaanderen) for a Ph.D. grant. This investigation has been supported by grants from the Concerted Research Action (G.O.A.), from the Inter-university Attraction Pool (IAP) program and from the Centre of Excellence at University of Leuven (CECAT).

References

[1] M. Iwamoto, H. Furukawa, Y. Mine, F. Uemura, S. Mikuriya, S. Kagawa, J. Chem. Soc., Chem. Commun. (1986) 1272–1273.
[2] J. Perez-Ramirez, F. Kapteijn, K. Schöffel, J.A. Moulijn, Appl. Catal. B 44 (2003) 117–151.
[3] M.A.G. Hevia, J. Perez-Ramirez, Appl. Catal. B 77 (2007) 248–254.
[4] B. Wichterlová, Z. Sobalik, J. Dedecek, Appl. Catal. B 41 (2003) 97–114.
[5] A.L. Yakovlev, G.M. Zhidomirov, R.A. van Santen, Catal. Lett. 75 (2001) 45–48.
[6] K. Tran, P. Kilpinen, N. Kumar, Appl. Catal. B 78 (2008) 129–138.
[7] P. Forzatti, Appl. Catal. A 222 (2001) 221–236.
[8] V.I. Pârvulescu, P. Grange, B. Delmon, Catal. Today 46 (1998) 233.
[9] Y. Li, J.N. Armor, Appl. Catal. B 1 (1992) L21–L29.
[10] R.S. da Cruz, A.J.S. Mascarenhas, H.M.C. Andrade, Appl. Catal. B 18 (1998) 223–231.
[11] J.A. Ryder, A.K. Chakraborty, A.T. Bell, J. Phys. Chem. B 106 (2002) 7059–7064.
[12] F. Kapteijn, J. Rodriguez-Mirasol, J.A. Moulijn, Appl. Catal. B 9 (1996) 25–64.
[13] F. Kapteijn, G. Marbán, J. Rodriguez-Mirasol, J.A. Moulijn, J. Catal. 167 (1997) 256–265.
[14] Y. Li, J.N. Armor, Appl. Catal. B 1 (1992) L31–L40.
[15] J.N. Armor, Catal. Today 26 (1995) 147–158.
[16] M. Iwamoto, H. Hamada, Catal. Today 10 (1991) 57–71.
[17] H. Chen, S. Shen, X. Chen, S. Kawi, Appl. Catal. B 50 (2004) 37–47.
[18] C.W. Lee, P.J. Chong, Y.C. Lee, C.S. Chin, L. Kevan, Catal. Lett. 48 (1997) 129–133.
[19] A. Jentys, A. Lugstein, H. Vinek, J. Chem. Faraday Trans. 93 (1997) 4091–4094.
[20] H. Ohtsuka, T. Tabata, O. Okada, L.M.F. Sabatino, G. Bellussi, Catal. Lett. 44 (1997) 265–270.
[21] S. Jong, S. Cheng, Appl. Catal. A 126 (1995) 51–66.
[22] X. Wang, H. Chen, W.M.H. Sachtler, Appl. Catal. B 26 (2000) L227–L239.
[23] X. Wang, H. Chen, W.M.H. Sachtler, Appl. Catal. B 29 (2001) 47–60.
[24] F. Seyedeyn-Azad, D. Zhang, Catal. Today 68 (2001) 161–171.
[25] M.C. Campa, S. De Rossi, G. Ferraris, V. Indovina, Appl. Catal. B 8 (1996) 315–331.
[26] J. Zhang, W. Fan, Y. Liu, R. Li, Appl. Catal. B 76 (2007) 174–184.
[27] T. Montanari, O. Marie, M. Daturi, G. Busca, Catal. Today 110 (2005) 339–344.
[28] T. Montanari, O. Marie, M. Daturi, G. Busca, Appl. Catal. B 71 (2007) 216–222.

[29] C. Resini, T. Montanari, L. Nappi, G. Bagnasco, M. Turco, G. Busca, F. Bregani, M. Notaro, G. Rocchini, J. Catal. 214 (2003) 179–190.
[30] X. Wang, H. Chen, W.M.H. Sachtler, J. Catal. 197 (2001) 281–291.
[31] M. Mihaylov, K. Hadjiivanov, Chem. Commun. (2004) 2200–2201.
[32] P. Pietrzyk, Z. Sojka, Chem. Commun. (2007) 1930–1932.
[33] D. Kaucký, A. Vondrová, J. Dedecek, B. Wichterlová, J. Catal. 194 (2000) 318–329.
[34] C. Chupin, A.C. van Veen, M. Konduru, J. Després, C. Mirodatos, J. Catal. 241 (2006) 103–114.
[35] A. Boix, E.E. Miró, E.A. Lombardo, M.A. Bañares, R. Mariscal, J.L.G. Fierro, J. Catal. 217 (2003) 186–194.
[36] G. Bagnasco, M. Turco, C. Resini, T. Montanari, M. Bevilacqua, G. Busca, J. Catal. 225 (2004) 536–540.
[37] M. Majdan, S. Pikus, M. Kowalska-Ternes, A. Gladysz-Plaska, H. Skrzypek, W. Kazimierczak, J. Mol. Struct. 657 (2003) 47–56.
[38] J. Dedecek, L. Capek, D. Kaucký, Z. Sobalík, B. Wichterlová, J. Catal. 211 (2002) 198–207.
[39] D. Kaucký, J. Dedecek, B. Wichterlová, Micropor. Mesopor. Mater. 31 (1999) 75–87.
[40] J. Dedecek, D. Kaucký, B. Wichterlová, Micropor. Mesopor. Mater. 35–36 (2000) 483–494.
[41] M. Mhamdi, E. Marceau, S. Khaddar-Zine, A. Ghorbel, M. Che, Y.B. Taarit, F. Villain, Catal. Lett. 98 (2004) 135–140.
[42] J. Janas, T. Machej, J. Gurgul, R.P. Socha, M. Che, S. Dzwigaj, Appl. Catal. B 75 (2007) 239–248.
[43] A.A. Verberckmoes, B.M. Weckhuysen, R.A. Schoonheydt, Micropor. Mesopor. Mater. 22 (1998) 165–178.
[44] K. Pierloot, A. Delabie, C. Ribbing, A.A. Verberckmoes, R.A. Schoonheydt, J. Phys. Chem. B 102 (1998) 10789–10798.
[45] A.B.P. Lever, Inorganic Electronic Spectroscopy, second ed., Elsevier, Amsterdam, 1984.
[46] R.G. Burns, Mineralogical Applications of Crystal Field Theory, second ed., Cambridge University Press, Cambridge, 1993.
[47] A. Martínez-Hernández, G.A. Fuentes, Appl. Catal. B 57 (2005) 167–174.
[48] C.M. de Correa, A.L. Villa, M. Zapata, Catal. Lett. 38 (1996) 27–32.
[49] P.J. Smeets, M.H. Groothaert, R.M. van Teeffelen, H. Leeman, E.J.M. Hensen, R.A. Schoonheydt, Stud. Surf. Sci. Catal. 170 (2007) 1080–1087.
[50] P.J. Smeets, M.H. Groothaert, R.M. van Teeffelen, H. Leeman, E.J.M. Hensen, R.A. Schoonheydt, J. Catal. 245 (2007) 358–368.
[51] P.J. Smeets, B.F. Sels, R.M. van Teeffelen, H. Leeman, E.J.M. Hensen, R.A. Schoonheydt, J. Catal. 256 (2008) 183–191.
[52] M.H. Groothaert, J.A. van Bokhoven, A.A. Battiston, B.M. Weckhuysen, R.A. Schoonheydt, J. Am. Chem. Soc. 125 (2003) 7629–7640.
[53] G.D. Pirngruber, P.K. Roy, R. Prins, J. Catal. 246 (2007) 147–157.
[54] K. Sun, H. Xia, Z. Feng, R. Van Santen, E. Hensen, C. Li, J. Catal. 254 (2008) 383–396.
[55] J. Perez-Ramirez, J. Catal. 227 (2004) 512–522.
[56] N. Hansen, A. Heyden, A.T. Bell, F.J. Keil, J. Catal. 248 (2007) 213–225.
[57] P.K. Roy, R. Prins, G.D. Pirngruber, Appl. Catal. B 80 (2008) 226–236.
[58] I. Melian-Cabrera, C. Mentruit, J.A.Z. Pieterse, R.W. van den Brink, G. Mul, F. Kapteijn, J.A. Moulijn, Catal. Commun. 6 (2005) 301–305.
[59] L. Obalova, V. Fila, Appl. Catal. B 70 (2007) 353–359.
[60] L. Capek, J. Dedecek, B. Wichterlová, J. Catal. 227 (2004) 352–366.
[61] J.A. van Bokhoven, D.C. Koningsberger, P. Kunkeler, H. van Bekkum, A.P.M. Kentgens, J. Am. Chem. Soc. 122 (2000) 12842–12847.
[62] Y.J. Li, J.N. Armor, J. Catal. 150 (1994) 376–387.
[63] H. Ohtsuka, T. Tabata, O. Okada, L.M.F. Sabatino, G. Bellussi, Catal. Today 42 (1998) 45–50.
[64] S.A. Beloshapkin, E.A. Paukshtis, V.A. Sadykov, J. Mol. Catal. A 158 (2000) 355–359.
[65] L.J. Lobree, A.W. Aylor, J.A. Reimer, A.T. Bell, J. Catal. 169 (1997) 188–193.
[66] A. Shichi, T. Hattori, A. Satsuma, Appl. Catal. B 77 (2007) 92–99.
[67] E. Ivanova, K. Hadjiivanov, D. Klissurski, M. Bevilacqua, T. Armaroli, G. Busca, Micropor. Mesopor. Mater. 46 (2001) 299–309.
[68] K. Hadjiivanov, B. Tsyntsarski, T. Nikolova, Phys. Chem. Chem. Phys. 1 (1999) 4521–4528.
[69] K. Gora-Marek, B. Gil, M. Sliwa, J. Datka, Appl. Catal. A 330 (2007) 33–42.